JOURNAL OF MATERIALS SCIENCE 23 (1988) 3692–3697

Creep crack propagation at elevated temperature in a heat-resistant steel

Z. B. CAO, P. E. LI*, J. S. ZHANG, S. J. ZHU
Materials Engineering Department, Dalian Institute of Technology, Dalian, China

The creep crack propagation behaviour of a 25 Cr–20 Ni heat-resistant steel at 1103 to 1163 K has been studied using a CT-specimen with a thickness of 3 to 9 mm. With increasing specimen thickness, the crack growth rates increase in the thickness range 6 to 9 mm but remain almost constant in the range 3 to 6 mm. The temperature dependence of crack growth rates can be related to a thermally activated process of creep crack propagation. A creep mechanism is suggested to be the rate controlling process of creep crack propagation. The activation energy of creep crack propagation increases with increasing stress intensity factor. The effect of microstructure on crack growth rates shows that the as-cast specimen has a much higher crack growth rate than specimens pre-aged for 1500 to 8000 h and the specimen aged for 5000 h has the optimum crack propagation resistance. The characteristics of creep crack propagation are explained by the variation of microstructure with ageing, especially the size, distribution and stability of secondary carbides and the morphology of eutectic carbides.

1. Introduction

Creep crack propagation behaviour of alloys has been a topic of considerable interest in the past two decades. This is because the failure of components used under creep conditions can occur by the propagation of a single macroscopic crack. Siverns and Price [1] first applied fracture mechanics to the study of creep rupture. Since then, creep crack propagation behaviour in a large variety of materials such as aluminium alloys, carbon steels, Cr–Mo–V steels, stainless steels and superalloys [2–6] has been studied both from materials and from engineering fracture mechanics aspects. But few data on creep crack propagation in the HK40 steel have been reported.

The HK40 steel is widely used for centrifugally-cast reformer tube in the steam reforming process in petrochemical plants. It is subjected to the operating conditions of high temperature (873 to 1273 K) and high pressure (2.9 to 3.5 MPa). After about one-quarter or one-third of the design life (10^5 h) under service, circumferential and longitudinal surface cracks formed inside the tube [7]. Statistics showed that the practical service term of a tube is about two-thirds or two-fifths of the design life and the failure of the great majority of tubes is caused by the propagation of creep cracks [8]. This means that the creep crack propagation occurs under operation during the latter half of the total service life of these tubes. Therefore, the study of creep crack propagation behaviour in the HK40 steel is of great importance for the prediction of the residual lifetime and the establishment of the renewal criteria of existing tubes.

Previous works [9–11] have shown that the characteristics of creep crack propagation depend on both material and microstructure, as well as being influenced by the test conditions such as temperature and specimen thickness.

This paper reports an examination of the effect of specimen thickness and temperature on creep crack propagation in the HK40 steel. Furthermore, the works on the effect of microstructure have been extended using the pre-ageing treatment.

2. Experimental procedure

The HK40 steel tubes used for this study are in the as-cast state (centrifugal) with an inside diameter of 110 mm and a wall thickness of 20 mm. The chemical composition of the steel falls within the ASTM standards, as shown in Table I.

The CT-specimen geometry for the creep crack propagation tests is shown in Fig. 1 (specimen 1 for tests of the effect of specimen thickness and temperature, specimen 2 for tests of the effect of microstructure). The specimen orientation in this figure is for the simulation of the practical longitudinal crack propagation in the tubes. The specimens are notched by an electrical spark machine with a root radius of 0.06 mm, without being fatigue precracked.

The crack propagation tests under constant load are carried out in a creep testing machine. The specimens are heated in a three-zone resistance wire-wound furnace. The test temperature is maintained with a stability of ± 3 K. The crack lengths are measured by a d.c. electrical potential drop technique. The values

TABLE I

C	Cr	Ni	Mn	Si	S	P	Mo
0.39	25.35	21.55	0.80	0.63	0.010	0.023	0.27

*All correspondence to be addressed to Dr Li Peien.

0022–2461/88 $03.00 + .12

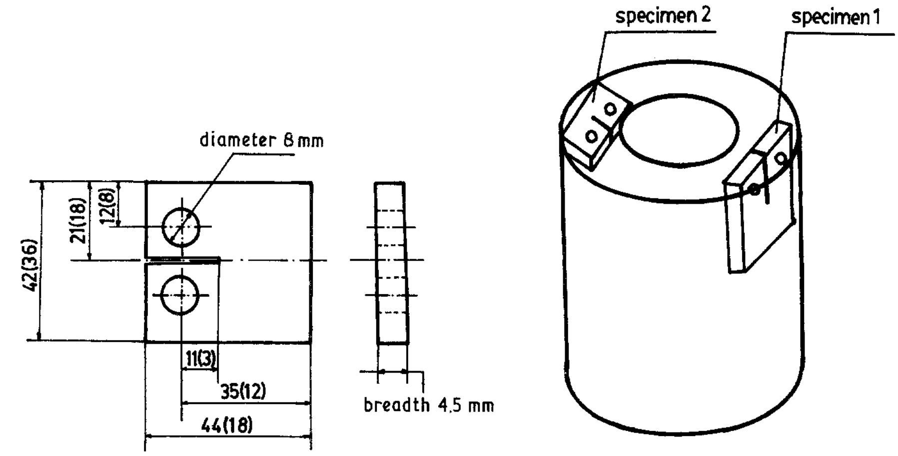

Figure 1 (a) CT-specimen dimensions (mm), (b) the location of specimens in a centrifugally-cast tube.

of load point displacement are read from an instrument attached to the testing machine.

Tests of the effect of specimen thickness on creep crack propagation have been carried out in specimens 3, 6 and 9 mm thick at 1144 K under a stress of 14.7 MPa. For the effect of temperature, the crack growth rates are measured at four temperatures within 1103 to 1163 K under a stress of 14.7 MPa using 3 mm thick specimens.

In order to develop the desired microstructures, the as-cast specimens were aged at 1144 K for 1500, 3000, 5000 and 8000 h. The stress and temperature for the tests of the effect of microstructure are 25.4 MPa and 1144 K, respectively.

3. Results and discussion

3.1. Effect of specimen thickness

Crack growth rates as a function of stress intensity factor, K_I, are shown in Fig. 2 for three different thicknesses. A remarkable increase in crack growth rates occurs when the specimen thickness increases from 6 to 9 mm at a constant K_I, though virtually no difference in crack growth rates exists between the 3 and 6 mm thick specimens.

Neate [4] has studied the effect of specimen thickness on the creep crack growth rates in a $\frac{1}{2}$Cr–$\frac{1}{2}$Mo–V steel. For the quenched specimens, the crack growth increases several times with increasing specimen thickness from 5 to 15 mm. For the normalized and tempered specimens, although the thickness increases from 5 to 25.4 mm, the crack growth rate is almost constant. However, in the case of the HK40 steel, there are different thickness ranges within which the specimen thickness can have either some or no influence on crack growth rates.

It is common for increasing specimen thickness to lead to a higher deformation constraint or more intense stress state in a region in front of the crack tip and this will cause geometric embrittlement in materials and a decrease of fracture toughness [12]. On the other hand, the degree of this deformation constraint in a region in front of the crack tip in a specimen varies with material [4]. In the HK40 steel, with increasing specimen thickness from 6 to 9 mm, a large change from the plane-stress to plane-strain state can take place. However, within the thickness range 3 to 6 mm the same plane-stress state prevails.

3.2. Effect of temperature

Crack growth rates varying with stress intensity factor at four temperatures are illustrated in Fig. 3.

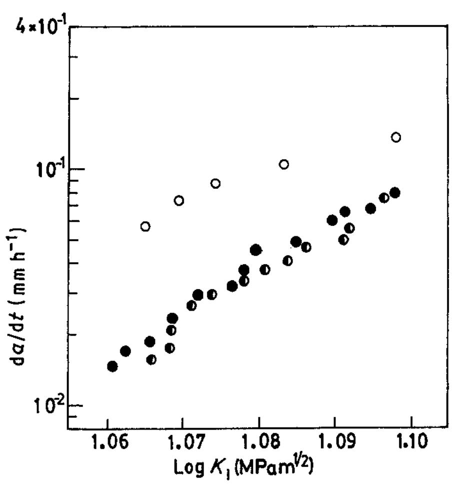

Figure 2 Effect of specimen thickness on the crack growth rate, da/dt, as a function of the stress intensity factor, K_I, at 1144 K. (○) 9 mm, (◐) 6 mm, (●) 3 mm.

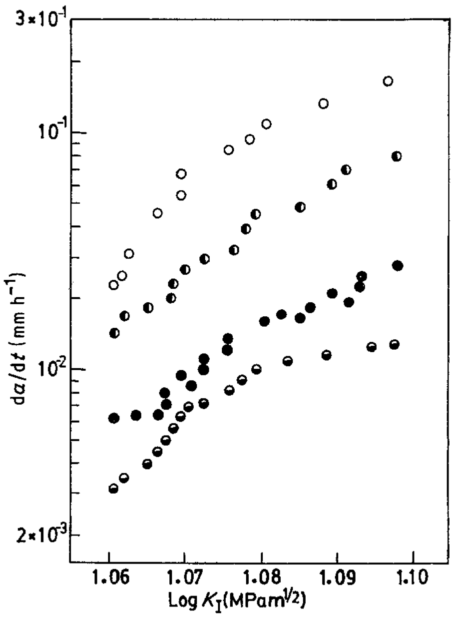

Figure 3 Effect of the temperature on the crack growth rate, da/dt, as a function of the stress intensity factor, K_I. (○) 1163 K, (◐) 1144 K, (●) 1123 K, (⊖) 1103 K.

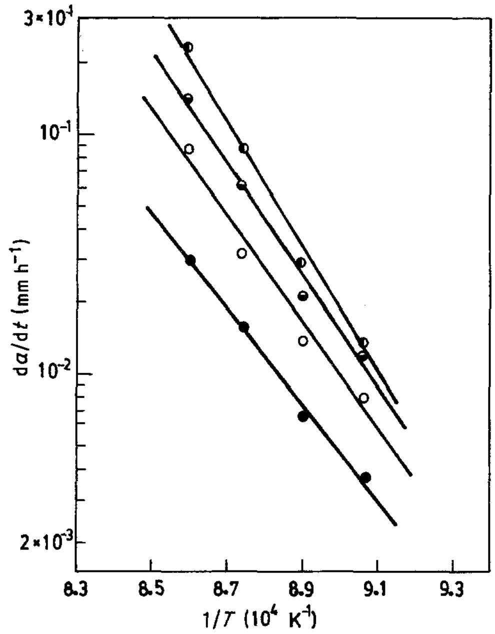

Figure 4 Arrhenius plot of the creep crack growth rate, da/dt, for calculating the activation energy of creep crack propagation. K_I (MPa $m^{1/2}$): (●) 11.55, (○) 11.90, (◒) 12.30, (◐) 12.65.

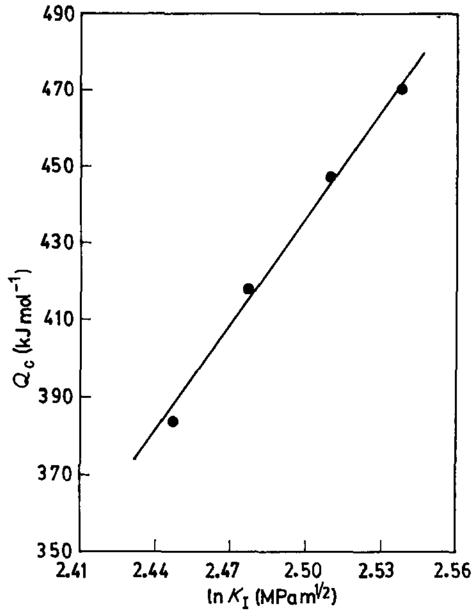

Figure 5 An experimental relation between the activation energy of creep crack propagation, Q_c, and the stress intensity factor, K_I.

The relation between the log crack growth rate, log (da/dt), and the reciprocal of absolute temperature, $1/T$, is plotted for a constant K_I, as shown in Fig. 4. The estimated values of apparent activation energy of creep crack propagation are 370 to 470 kJ mol^{-1} for a stress intensity factor varying from 11.55 to 12.65 MPa $m^{\frac{1}{2}}$. These values are close to the calculated creep activation energies of 352 to 485 kJ mol^{-1} according to the data given by Roach and Vanecho [13] for the HK40 steel at 1103 to 1255 K. This suggests that a creep mechanism can be rate controlling for creep crack propagation.

A plot of the activation energy of creep crack propagation against the log stress intensity factor is shown in Fig. 5. It is of interest to note that the activation energy of creep crack propagation increases with an increase of stress intensity factor. This is in contrast to Yokobori's result of a decrease in activation energy with an increase of stress intensity factor [14]. On the other hand, Floreen [15] pointed out that the activation energy of creep crack propagation is independent of stress intensity. It should be noted that in the case of the as-cast HK40 steel there is a continuous precipitation of carbides in the matrix during crack propagation. This was different from the two cases mentioned above. It is considered that the experimental relationship in Fig. 5 is related to the precipitation of carbides. Moreover, it is also found that the creep activation energy is proportional to the applied stress in the HK40 steel.

3.3. Effect of microstructure

Fig. 6 shows the microstructure of the as-cast and aged specimens. The cast microstructure consists of γ matrix and $\gamma + M_7C_3$ eutectic. After ageing at 1144 K, the non-homogeneous precipitation of secondary carbides $M_{23}C_6$ takes place in the matrix of the HK40 steel [16]. The non-homogeneous precipitation of carbides caused by the segregation of alloying elements (mainly carbon and chromium) during solidification makes a so-called carbide "segregation band" formed at the dendritic cell boundaries. It has been shown that the nucleation of carbides in the "segregation band" is very fast followed by the coarsening of carbides. However, the precipitation of carbides in the central region of the dendritic cells is slow due to lower supersaturation of alloying elements in this region. It has been

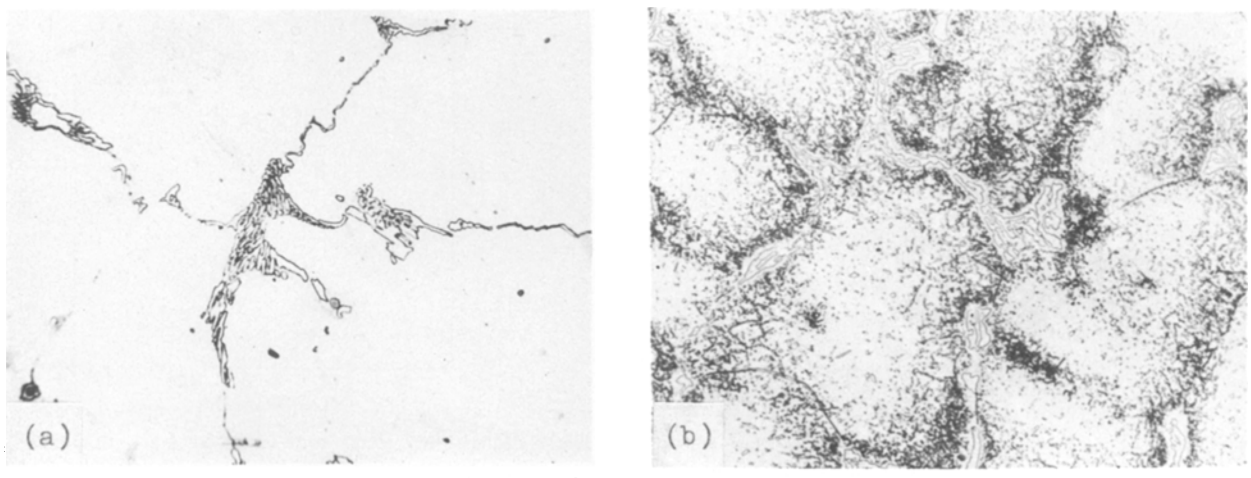

Figure 6 Microstructure of the as-cast and pre-aged specimens: (a) as-cast, (b) 1500 h, (c) 3000 h, (d) 5000 h, (e) 8000 h.

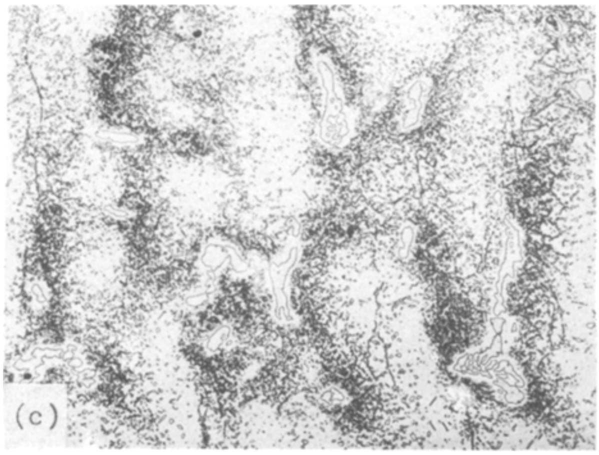

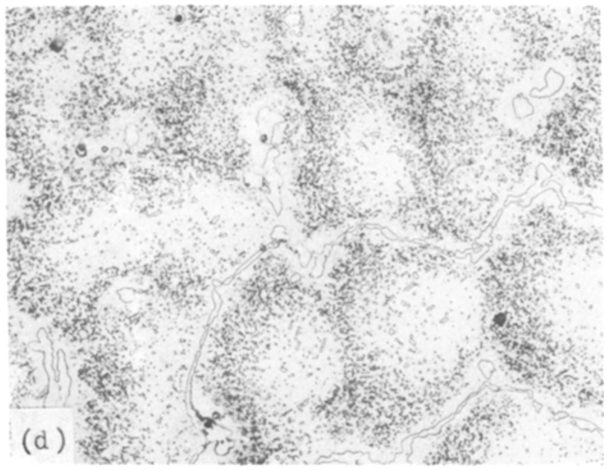

Figure 6 Continued.

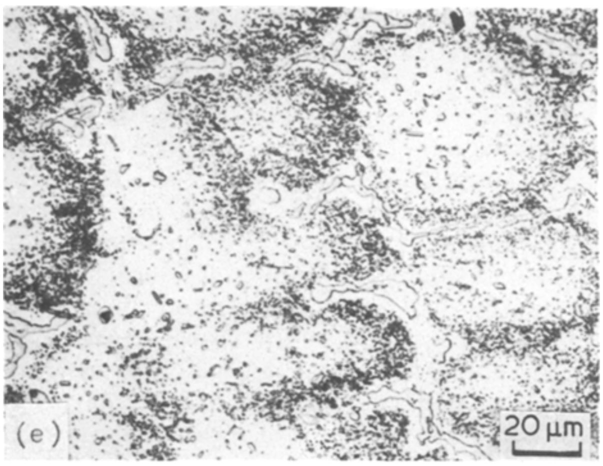

observed that the size of secondary carbides in the "segregation band" become evidently larger when the ageing time increases from 1500 to 8000 h. It should be noted that the specimen aged for 8000 h has much coarser carbide particles in the central region of the dendritic cells than the others (Fig. 6).

Fig. 7 shows the variation of the average Vicker's hardness, H_v, within the grains, measured in the fractured specimens, with ageing time. There is a monotonic decrease in the Vicker's hardness with ageing time. The variation of the parameter Hmc/Hmm, measured in the same specimens, with ageing time is also shown in Fig. 7. The parameter Hmc/Hmm is defined as a ratio of the microhardness in the "segregation band" to that in the central region of a dendritic cell. Hmc/Hmm is related to both the distribution of secondary carbides and the precipitation and coarsening velocity of secondary carbides in the different region of the dendritic cells. The coarsening of carbides and softening of matrix in the "segregation band" compared with the precipitation strengthening of carbides in the central region of the dendritic cells with the increase of ageing time make the ratio Hmc/Hmm decrease to a minimum at 5000 h. But then Hmc/Hmm increases again at 8000 h due to the severe coarsening of carbides in the central region of the dendritic cells (Fig. 6).

Creep crack growth rates are plotted against stress intensity factor for various heat-treated specimens in Fig. 8. It is observed that the crack growth rates of the as-cast specimen are 5 to 20 times higher than those of the pre-aged specimens within the range of stress intensity factor examined. This means that the crack

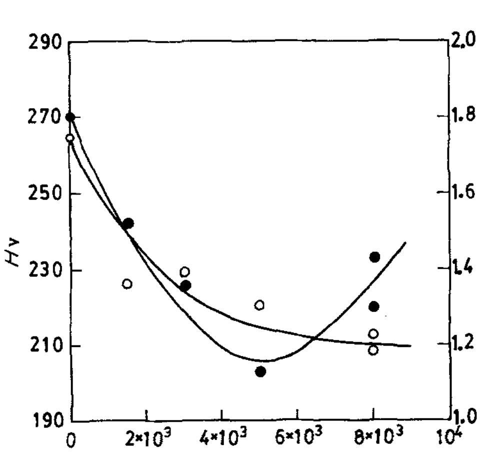

Figure 7 Variation of the Vicker's hardness, H_v (○) 5 kg, and the ratio, Hmc/Hmm (●), with ageing time, t.

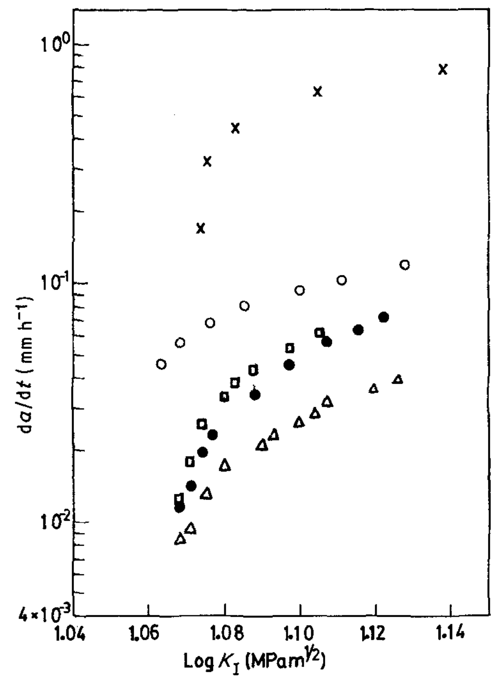

Figure 8 Effect of pre-ageing on the crack growth rate, da/dt, as a function of the stress intensity factor, K_I. (×), As-cast, (○) 1500 h, (□) 3000 h, (△) 5000 h, (●) 8000 h.

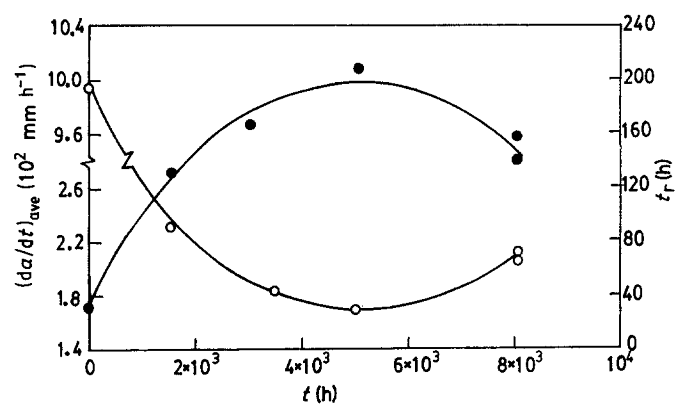

Figure 9 Variation of average crack growth rate $(\mathrm{d}a/\mathrm{d}t)_{\mathrm{ave}}$ (○), and the time to rupture, t_r (●), with ageing time, t.

propagation resistance in the as-cast HK40 steel is remarkably improved by pre-ageing. The higher crack growth rates of the as-cast specimen are produced because the continuous carbide precipitation in the matrix [16] renders the stress relaxation in a region in front of the crack tip more difficult.

Fig. 9 shows the relations between the average crack growth rate $(\mathrm{d}a/\mathrm{d}t)_{\mathrm{ave}}$, or the time to rupture, t_r, and the ageing time. It clearly illustrates the fast or slow crack propagation in various specimens. It can be seen that the specimen aged for 5000 h has the minimum average crack growth rate and the longest time to rupture. This suggests that there exists an optimum resistance to crack initiation and propagation at the ageing time of 5000 h.

Fig. 10 shows the variation of the critical load point displacement, δ_c, and the minimum load point displacement rate, $\dot{\delta}_{\min}$, with the ageing time. Li [17] has pointed out that δ_c can be used to characterize the creep ductility and $\dot{\delta}_{\min}$ the creep deformation rate in the local zone in front of the crack tip. It can be seen that δ_c and $\dot{\delta}_{\min}$ in general increase with ageing time. Fig. 11 demonstrates that $\dot{\delta}_{\min}$ has no monotonic relation with the time to rupture. The longest time to rupture is obtained at a $\dot{\delta}_{\min}$ or a proper local creep deformation rate in the crack tip region in the specimen aged for 5000 h.

The steady state creep crack propagation may be regarded as a kinetic balance of two or more competing processes: processes that promote the crack propagation such as creep deformation damage, void nucleation and growth, as well as grain-boundary sliding; processes that inhibit the crack propagation such as crack-tip blunting and stress relaxation by matrix deformation. From previous results, the creep crack propagation behaviour in various specimens can be explained by the change of microstructure occurring during pre-ageing. It has been noted that there is an intergranular crack growth mode in all the specimens. Thus, it is required that the deformation within grains coordinates with the grain-boundary sliding when cracks propagate along grain boundaries. With the increase of ageing time to 5000 h, the increase of the creep ductility and local creep deformation rates in the crack tip zone (Figs 10 and 11) by the coarsening of carbides in the "segregation band" make the stress concentration ahead of crack tip relax rapidly. Only small cavitation damage ahead of crack tip occurs due to the precipitating strengthening of the carbides in the central region of the dendritic cells. In addition, a small amount of eutectic carbide with a skeleton-like shape plays some role in retarding the grain-boundary sliding. As a result, the crack growth rates gradually decrease on increasing the ageing time to 5000 h. However, when the ageing time is longer than 5000 h such as 8000 h, the crack growth rates again increase. This is because the coarsening of secondary carbides in the dendritic cells weakens both the matrix and the grain boundaries, and consequently causes severe cavitation in the crack-tip zone. It is difficult for stress relaxation to compensate for the reduction of the failure strength in the crack tip zone. As a result, some loss in crack propagation resistance results in the specimen aged for 8000 h.

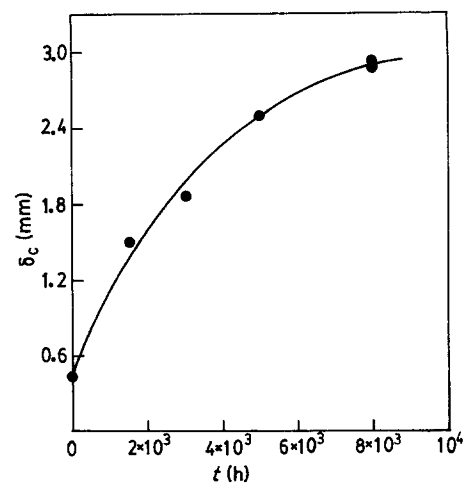

Figure 10 Variation of the critical load point displacement, δ_c, with ageing time, t.

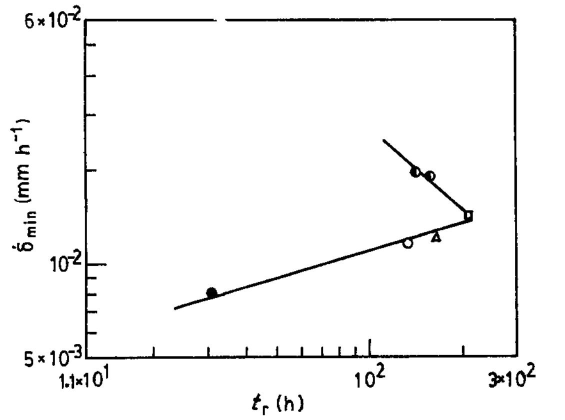

Figure 11 Relation between the minimum load point displacement rate, $\dot{\delta}_{\min}$, and the time to rupture, t_r. Ageing time: (●) as-cast, (○) 1500 h, (△) 3000 h, (□) 5000 h, (◐) 8000 h.

4. Conclusions

1. Specimen thickness has different effects on the creep crack growth rates in different thickness ranges in the HK40 steel. Crack growth rates increase on increasing the thickness from 6 to 9 mm but remain almost constant in the range 3 to 6 mm.

2. A creep mechanism could be the rate-controlling process of creep crack propagation. The activation energy of creep crack propagation increases with increasing stress intensity factor.

3. The creep crack propagation behaviour is strongly influenced by microstructure. The as-cast specimen has a much higher crack growth rate than the pre-aged specimens. After ageing, the creep crack propagation resistance of the as-cast HK40 steel has been improved.

4. Before ageing for 5000 h, the ageing treatment increases the ductility of the steel, and therefore raises the resistance to crack initiation and propagation. However, ageing over 5000 h, such as 8000 h, will reduce the failure strength in a region in front of the crack tip, thus increasing crack growth rates and decreasing the time to rupture.

References

1. M. SIVERNS and A. T. PRICE, *Nature* **228** (1970) 960.
2. V. M. RADHAKRISHNAN and A. J. McEVILY, *J. Eng. Mater. Tech. Trans. ASME* **102** (1980) 200.
3. S. TAIRA, R. OHTANI and T. KITAMURA, *ibid.* **101** (1979) 156.
4. G. J. NEATE, *Eng. Fract. Mech.* **9** (1977) 297.
5. K. OHJI, *Theoret. Appl. Mech.* **27** (1977) 3.
6. R. B. SCARLIN, *Mater. Sci. Engng* **30** (1977) 55.
7. F. G. WANG and Z. B. CAO, *J. Dalian Inst. Technol.* **21** (4) (1982) 165 (in Chinese).
8. K. KASAHARA, *Tetsu-to-Hagane* **65** (1979) 975 (in Japanese).
9. D. J. GOOCH, *Mater. Sci. Engng* **27** (1979) 57.
10. J. M. LARSON and S. FLOREEN, *Metall. Trans. A* **8** (1977) 51.
11. H. F. MERRICK and S. FLOREEN, *ibid.* **9** (1978) 231.
12. D. BROEK, "Elementary Engineering Fracture Mechanics" (Noordhoff, Leyden, 1974) p. 179.
13. D. B. ROACH and J. A. VANECHO, ASTM STP756 (American Society for Testing and Materials, Philadelphia, Pennsylvania, 1982) p. 275.
14. T. YOKOBORI, H. SAKATA and A. T. YOKOBORI Jr, *Eng. Fract. Mech.* **13** (1979) 533.
15. S. FLOREEN, *Metall. Trans. A* **6** (1975) 1741.
16. G. W. QIAO, D. H. WANG and Z. B. CAO, *Acta Metall. Sinica* **22** (1986) A345 (in Chinese).
17. LI PEIEN and CAO ZHIBEN, *Chinese J. Met. Sci. Tech.* **4** (1988) 69.

Received 9 June
and accepted 20 August 1987